Non-uniform imaging (continued)

SINA 2010/11

Logpolar mapping

$$w = f(z) = \log_a(z), \quad w, z \in C$$

$$z = x + iy = r(\cos\varphi + i\sin\varphi)$$

$$w = \rho(z) + i\,\vartheta(z)$$

$$z = re^{i\varphi}$$

$$\begin{cases} \rho = \log_a r \\ \vartheta = h\varphi \end{cases}$$

Geometrical interpretation

$$\begin{cases} \eta = q\vartheta \\ \xi = \log_a \frac{\rho}{\rho_0} \end{cases}$$

ρ and ϑ are the standard polar coordinates

$$\begin{cases} x = \rho\cos\vartheta \\ y = \rho\sin\vartheta \end{cases}$$

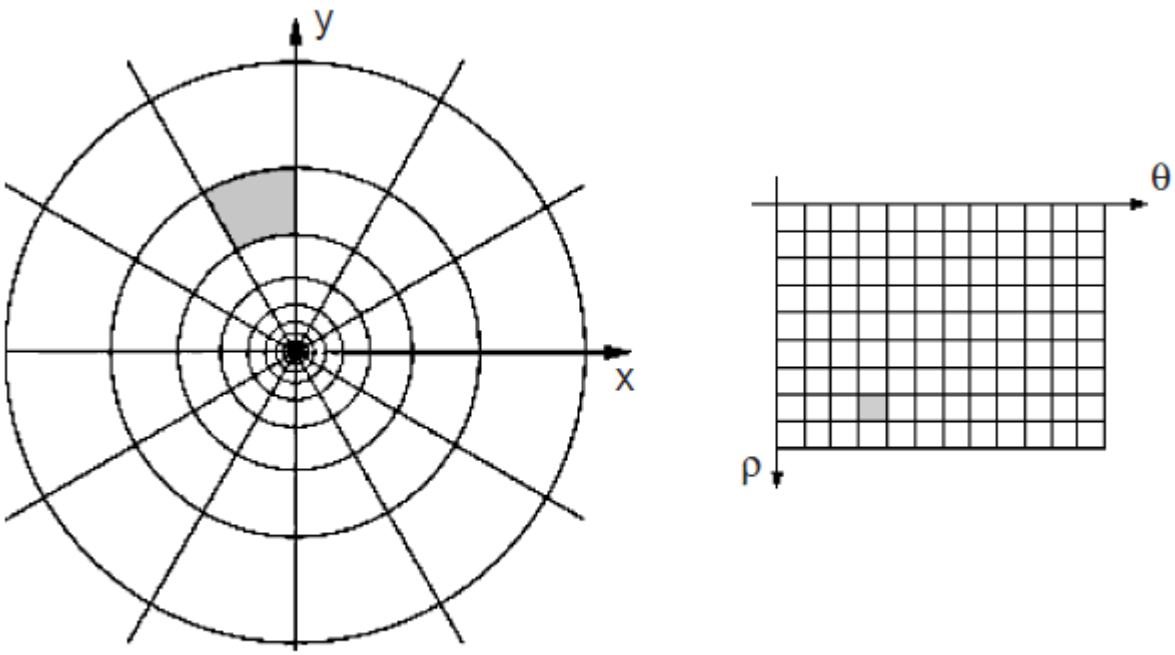

(a) (b)

Properties

- Conformal mapping, proximity
  - Use of local operators
- Scale change
  - Translation along the real axis
- Rotation change
  - Translation along the imaginary axis
- Translations
- Fourier-Mellin Transform

Angle preservation

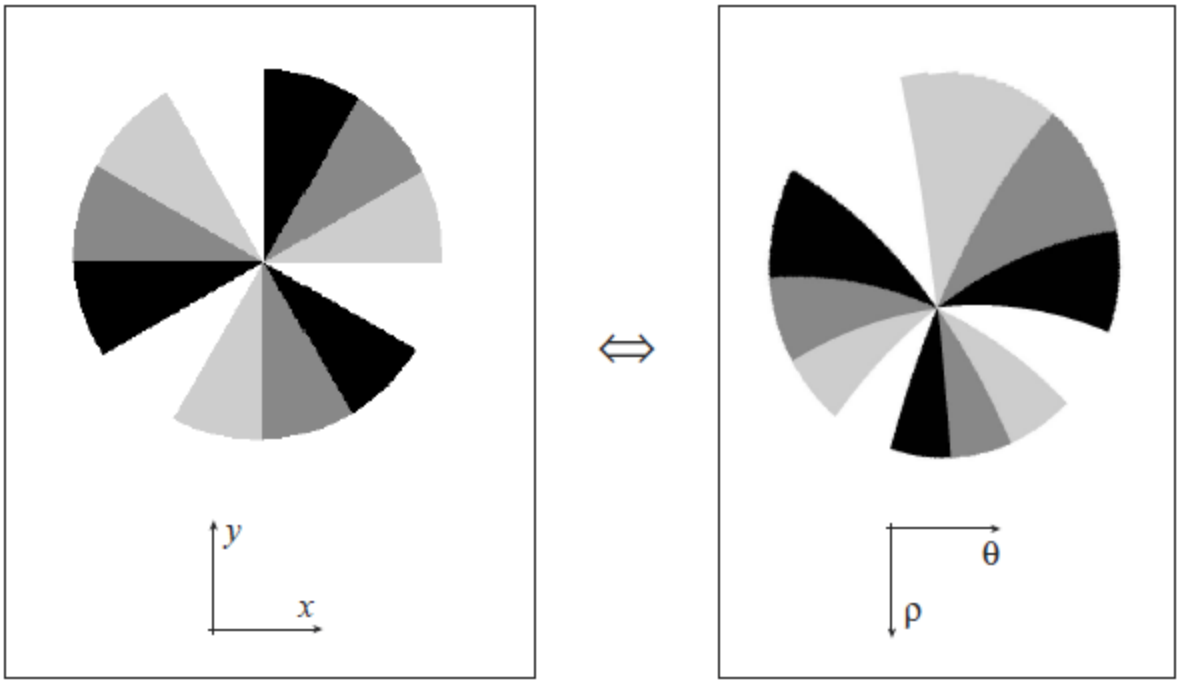

Figure 4.1. Angle Preservation: The angles are locally preserved after a log-polar Transformation. (a) Cartesian domain. (b) log-polar domain. Please note that both images a and b are particulars, so the origin of the mapping falls outside of the cartesian image.

Scale

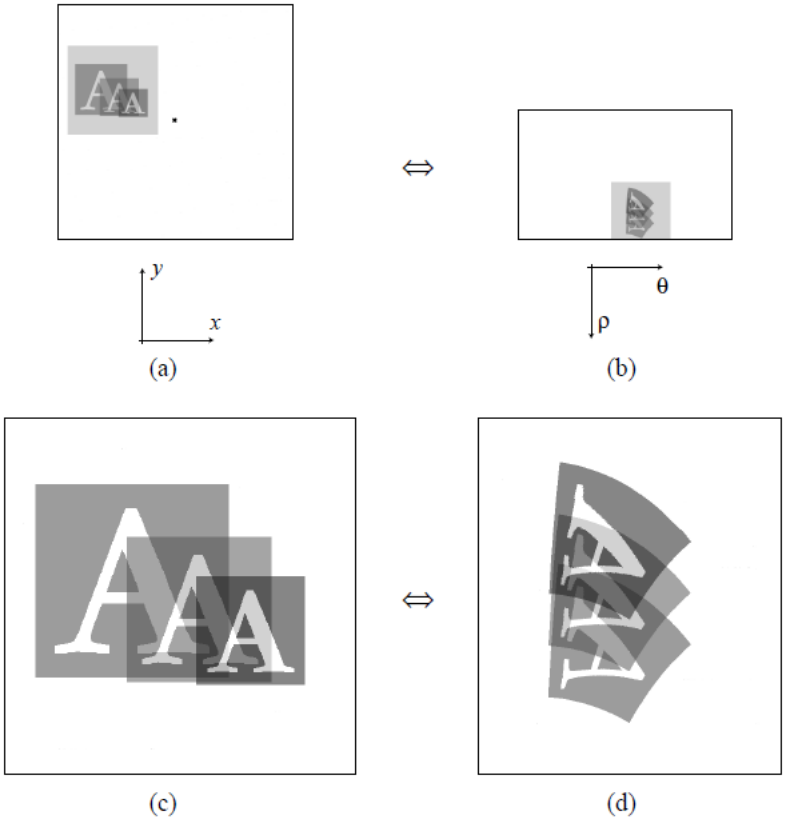

Figure 4.2. Scale Change: A pure scale change referred to the origin of the mapping, with no translational components, becomes a pure translation after the log-polar transform. (a) Cartesian domain. (b) log-polar domain. (c), (d) Enlargement of the shaded areas respectively in (a) and (b).

Rotation invariance

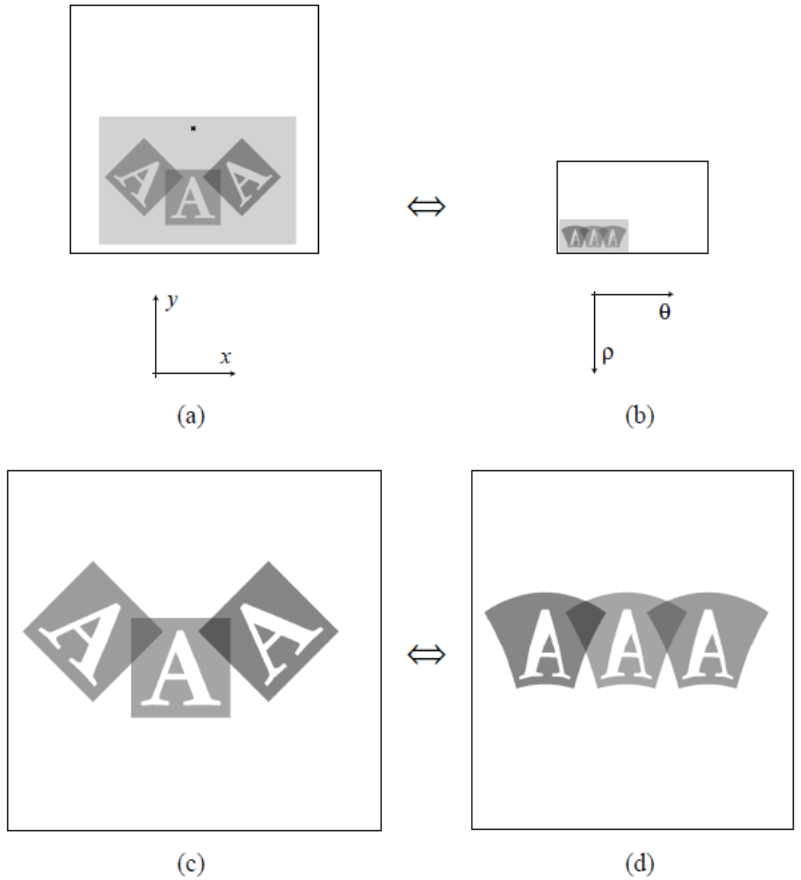

Figure 4.3. Rotation: A pure rotation referred to the origin of the mapping, with no translational components, becomes a pure translation after the log-polar transform. (a) Cartesian domain. (b) log-polar domain. (c), (d)Enlargement of the shaded areas respectively in (a) and (b).

Examples of rot-scale invariance

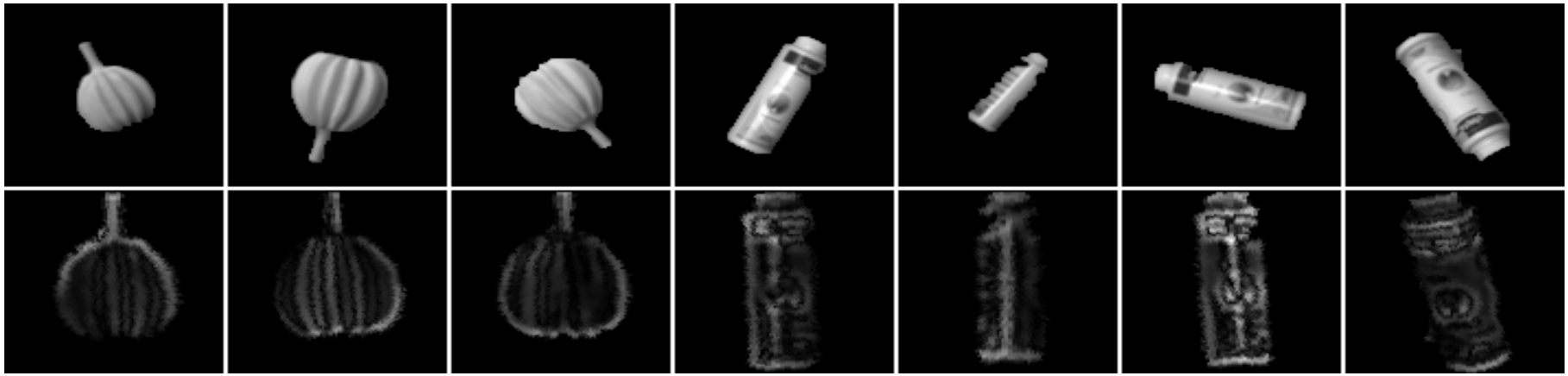

Translations

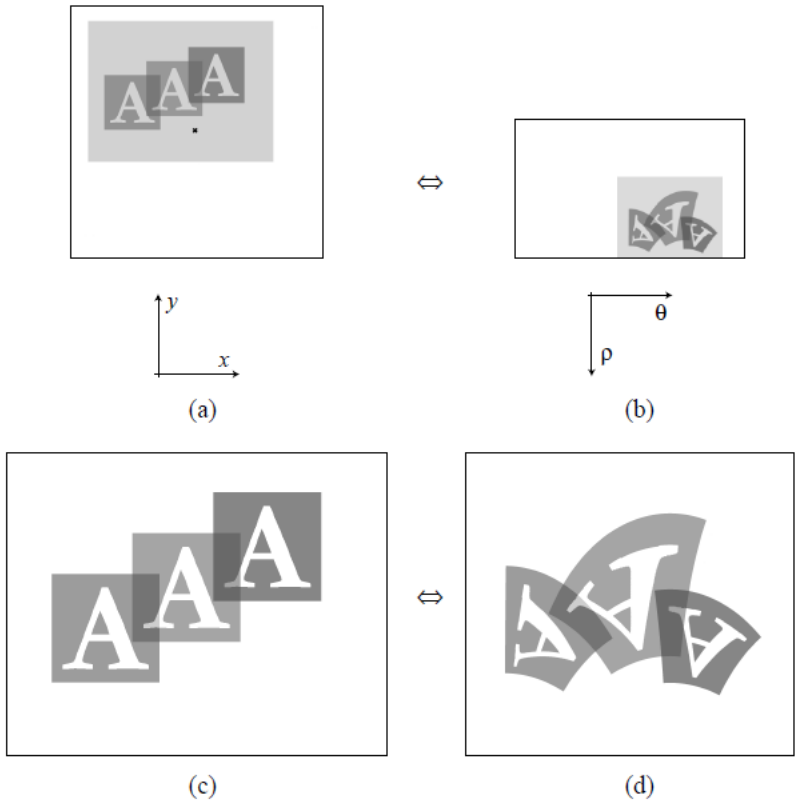

Figure 4.4. Translation: A pure translation implies a deformation of the object after the log-polar transform. (a) Cartesian domain. (b) log-polar domain. (c), (d) Enlargement of the shaded areas respectively in (a) and (b).

Fourier-Mellin transform

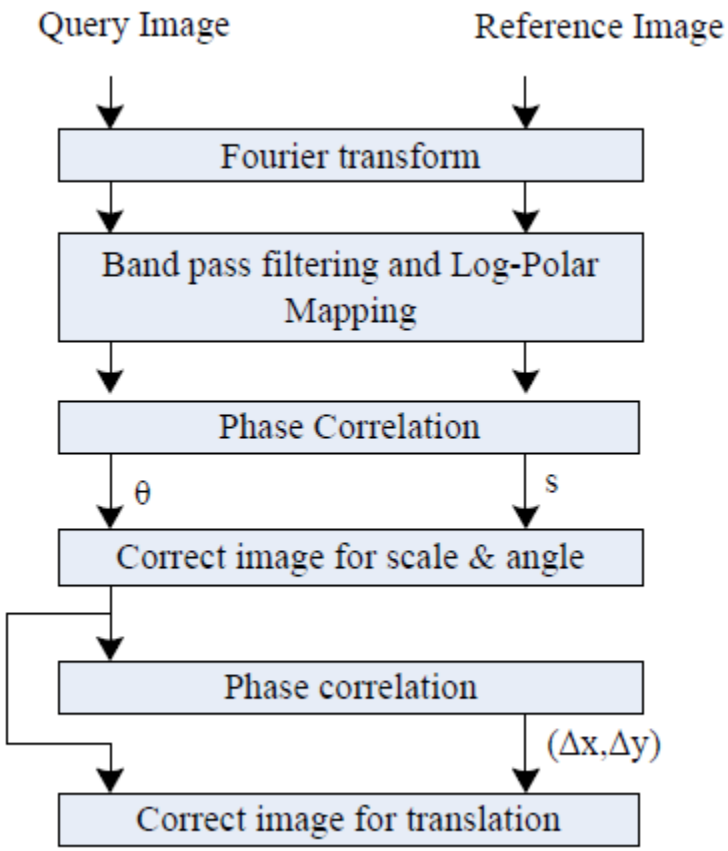
Query Image
Reference Image
Fourier transform
Band pass filtering and Log-Polar Mapping
Phase Correlation
θ
s
Correct image for scale & angle
Phase correlation
(Δx,Δy)
Correct image for translation

FMT-based optical flow

(a) Frame 14

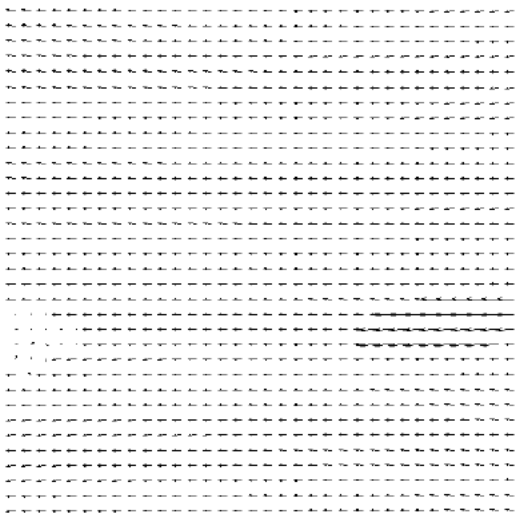

(b) Ground Truth

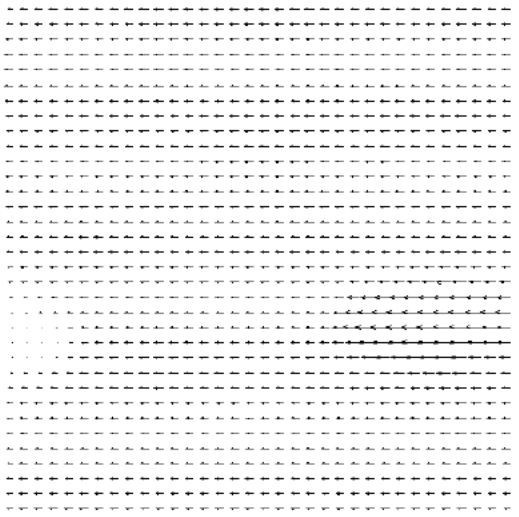

(c) Proposed FMT method

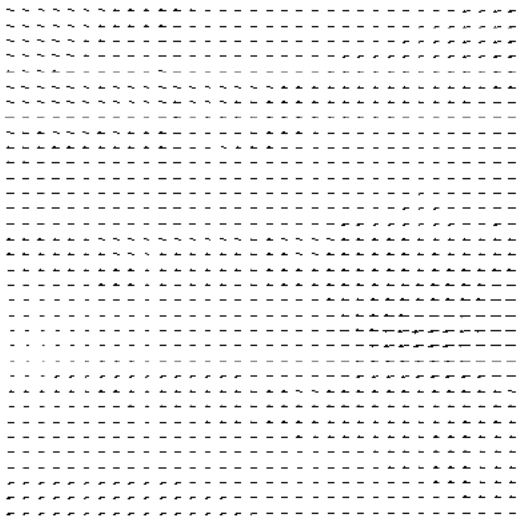

(d) Bruhn *et al.*

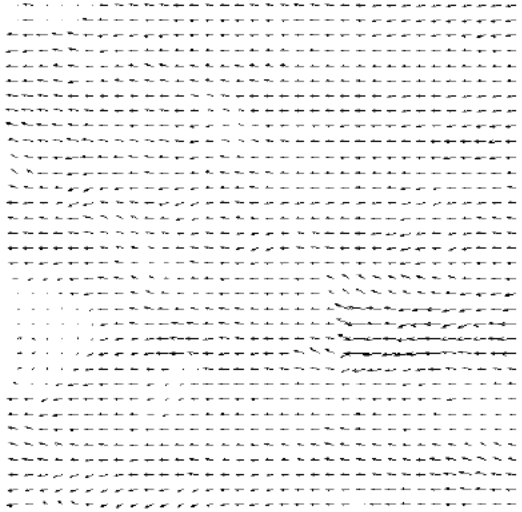

(e) Lucas-Kanade

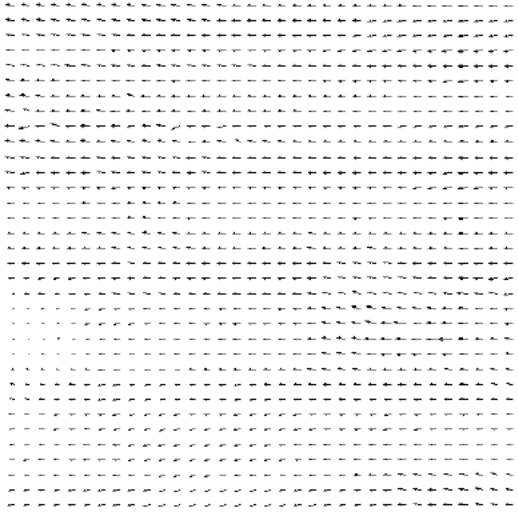

(f) Proesmans *et al.*

(a) Frame 10

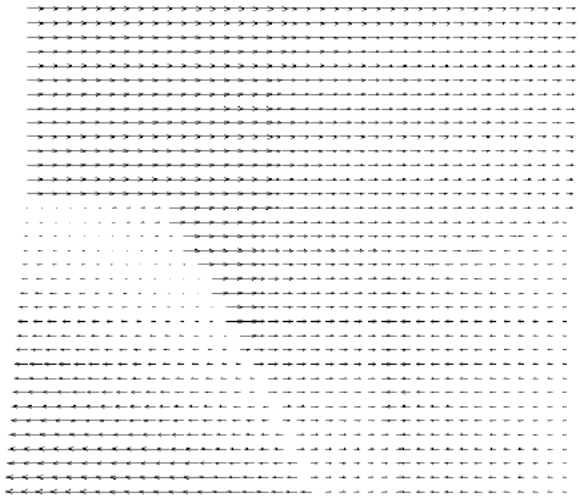

(b) Ground Truth

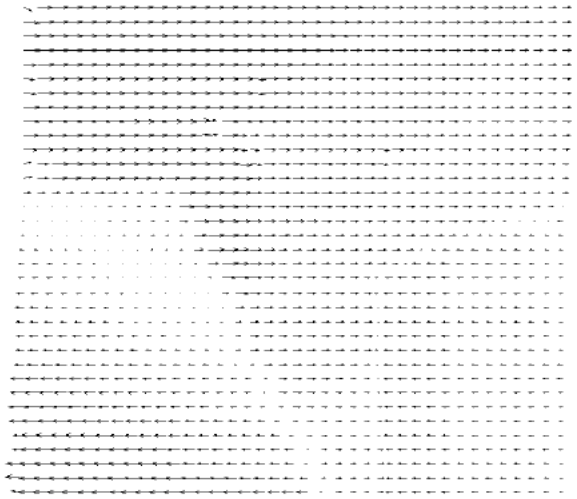

(c) Proposed FMT method

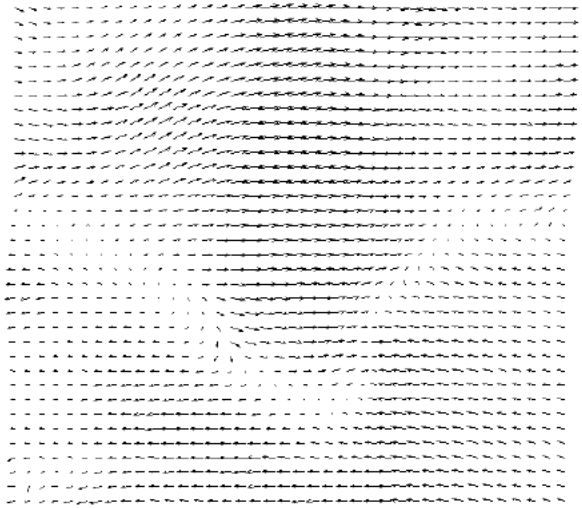

(d) Bruhn *et al.*

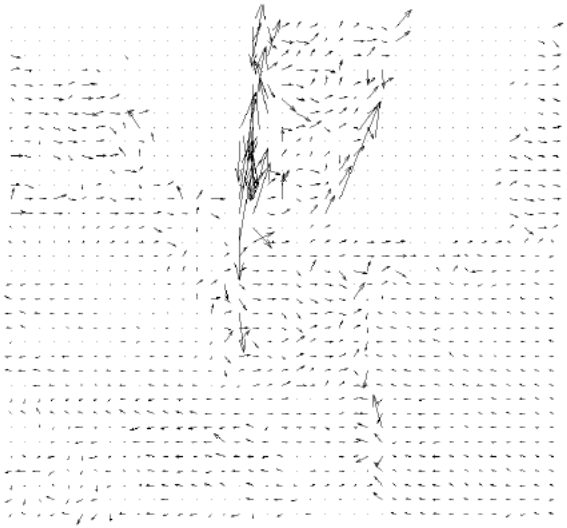

(e) Lucas-Kanade

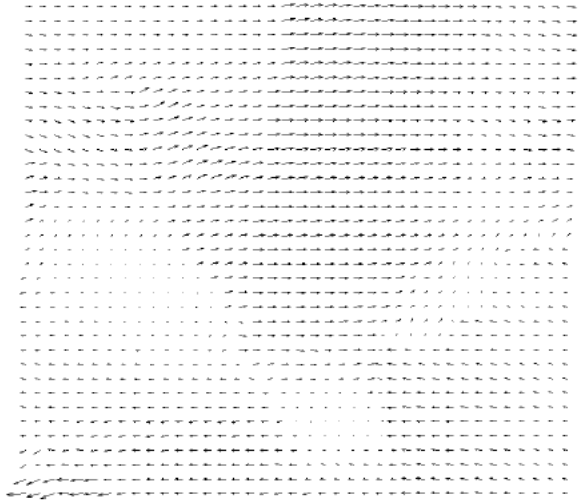

(f) Proesmans *et al.*

Method	Street		Venus		RubberWhale		Dimetrodon		Hydrangea	
	AAE	AME	AAE	AME	AAE	AME	AAE	AME	AAE	AME
Lucas-Kanade	6.45°	0.18	41.27°	0.74	18.69°	0.46	37.14°	0.66	29.85°	0.81
Proesman *et al.*	6.31°	0.17	18.25°	0.45	17.43°	0.38	22.23°	0.50	21.49°	0.82
2D-CLG	4.75°	0.15	19.38°	0.45	16.75.°	0.37	18.59°	0.40	27.87°	0.81
FMT (proposed)	4.66°	0.14	5.51°	0.14	10.07°	0.26	7.33°	0.18	11.83°	0.56

Table 1: Comparison of AAE and AME error metrics for different methods on synthetic and real image sequences

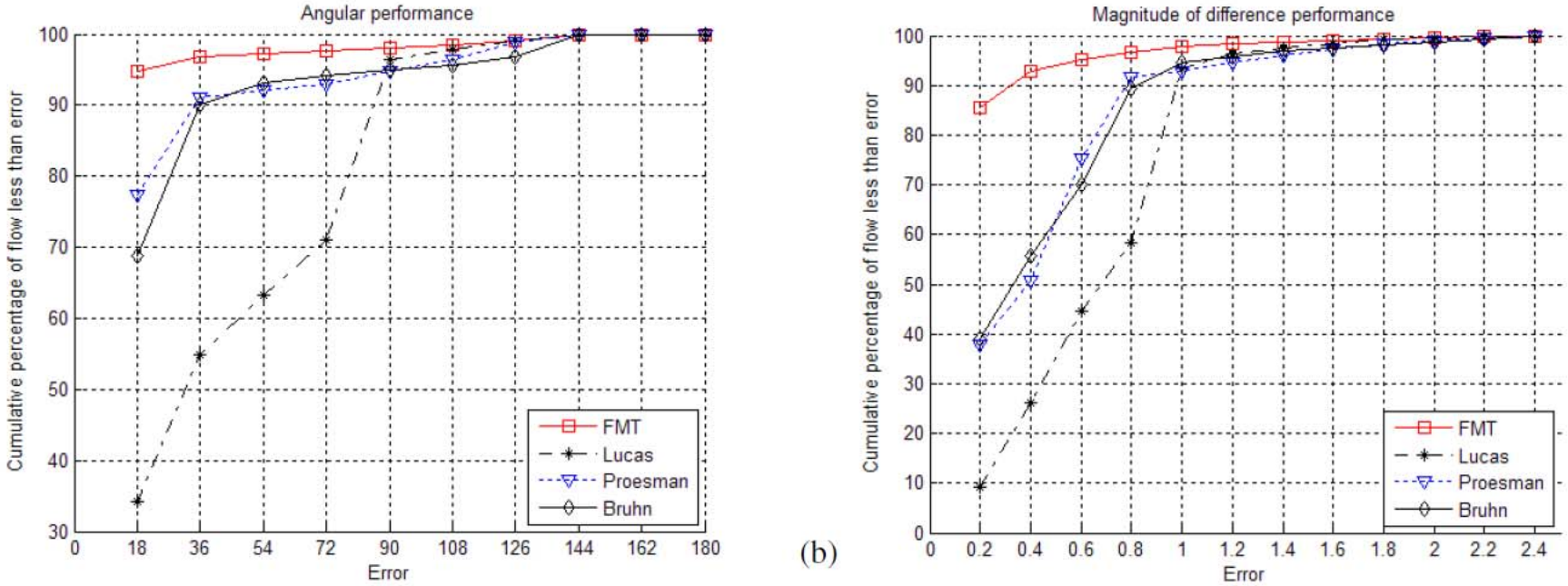

Figure 4: Performance comparison of four algorithms including the proposed FMT approach on the *Venus* sequence. Cumulative histograms for (a) average angular error and (b) average magnitude of difference error.